



# Aerodynamic simulation of rough and eroded blades, AEP effect and mitigation using low drag vortex generators

David Bretos-Arguiñena<sup>1</sup> and Beatriz Méndez-López<sup>1</sup>

<sup>1</sup>Wind Energy Department, Centro Nacional de Energías Renovables (CENER), Sarriguren, Spain

**Correspondence:** David Bretos-Arguiñena(dbretos@cener.com)

**Abstract.** Blade roughness depositions or blade erosion have an unquestionably effect over blade aerodynamics and wind turbine power production. This work is focused on the simulation using Computational Fluid Dynamics (CFD) of the NACA 63<sub>3</sub>418 airfoil with high roughness values and with different erosion typologies (pits and extreme losses of material). The CFD code used is OpenFOAM v8 and different technologies are selected to create the meshes to capture properly geometries' defects (ICEMCFD and ANSYS Workbench).

This study goes a step further by using low drag Vortex Generators (VGs) to mitigate the roughness and erosion harmful effects. Low drag VGs are compared with conventional ones and afterwards 3D blade sections are computed with roughness and erosion incorporating low drag VGs to evaluate the blade performance recovery achieved by the use of VGs. Finally, the impact of the different configurations (rough , eroded , rough + VG and eroded + VG) over Annual Energy Production (AEP) is evaluated on a virtual 2.5 MW wind turbine. The most important finding of the work presented in this paper is that AEP losses due to the existence of blade surface roughness or erosion can be recovered from the use of VGs up to 1.5 %.

## 1 Introduction

Wind turbine blade surface can be degraded during operation by different levels of roughness produced by air particles contamination or initial phases of blade erosion. Even though the effect of roughness over the airfoil performance has worried researchers and industry during the last 20 years, the 2D quantification of the effect that high roughness levels has over airfoil performance is still unresolved. With regard to erosion, there is not a standardized methodology to estimate its effect over airfoil performance or wind turbine AEP.

Roughness distribution on airfoil surface affects its performance by degrading the airfoil aerodynamic behaviour. If rough elements are located near the leading edge zone they influence the laminar to turbulent transition process moving upwards the transition point. On the other hand, roughness also modifies the flow characteristics in fully turbulent flows. Both effects are often confused with each other and the second is sometimes ignored. The deposition of big roughness elements on the blade surface is considered equivalent to the first stages of blade erosion. In addition, the growing installation of offshore wind farms



and the aim of reducing the cost of energy lead to the necessity of predicting accurately the energy losses due to rough or eroded blades in order to decide when to undertake wind turbine erosion control strategies or blade repairs.

The accurate prediction of the effect of surface roughness over the airfoil aerodynamic behaviour is of great interest for engineers, specially for the design of wind turbine blades. Aerodynamic predictions of airfoils sensitivity to roughness is an extremely challenging issue. Standish et al. (2012) performed experiments and simulations of a non specified airfoil of 18% thickness. The simulations were made using ANSYS CFX and roughness effects were accounted for by introducing an equivalent sand-grain roughness on surface patches. Afterwards AEP was calculated to evaluate the effect of roughness on power production. Normalized mechanical power output relative to measured power at two operational points below rated power of the SWT-2.3-93 wind turbine lead to power output reduction in 6 % and 7 %. Ehrmann et al. (2013) presented a study on the effect of leading edge roughness effect on airfoil performance. Different roughness types were characterized through measurements with laser scans on in-service wind turbine blades to perform wind tunnel simulations of a NACA 63<sub>3</sub>418 airfoil. The study was completed with computations using the flow solver OVERFLOW with a roughness amplification model for the Langtry-Menter transition model implemented. Differences between drag were observable between the clean and paint roughness configurations. More recently, further research has been done on the the field. Bak et al. (2020) studied the influence of the wind characteristics on the power production loss due to the existence of imperfections on the airfoil surface. It was concluded that the relative AEP losses due to leading edge damages reduced with increasing average wind speed on sites. For the low wind speed site the losses were between 1 % and 4 % depending on the extent and the type of the blade damage. For the high wind speed site the losses were between 0.5 % and 3 %. Furthermore, the bigger the extent of the damages the bigger the losses were. In addition, it was shown that increasing the maximum tip speed increased AEP and decreased the losses. Maniaci et al. (2020) focused their studies on reducing the uncertainties and AEP losses of 3% were reported when erosion is present in the National Rotor Testbed. Kruse et al. (2020) published CFD simulations of the NACA 63<sub>3</sub>418 and compared with experiments both with sandpaper and zz tape. Roughness was simulated with the Knopp model and the main conclusion was that not the lift decrease neither the drag increase were well captured. More recently, the authors of this paper presented detailed simulations of the NACA 63<sub>3</sub>418 using OpenFOAM Méndez and Pires (2022) for several roughness values and compared them with the wind tunnel experiments performed in the Second Call of Joint Experiments project described in Pires (2018).

Moving on to the study of blade erosion effect over airfoil performance simulations some work has been performed in recent years. Kruse et al. (2021) evaluated the NACA 63<sub>3</sub>418 airfoil with 1000 different protuberances in the airfoil leading edge ,the main conclusion was that position and the depth/height of the disturbance, with up to 35% lift reduction and 90% lift/drag reduction within the specified angle of attack (AoA) and disturbance parameter ranges. Campobasso et al. (2022) presented a study in which large and sparse erosion cavities were simulated in a DU96W180 airfoil for a Reynolds number of  $1.5 \cdot 10^6$ . It was found that the considered cavities can trigger transition, indicating the necessity of both resolving their geometry in the simulations and also modeling distributed surface roughness, since it affects the boundary layer characteristics and may trigger transition over the entire spanwise length affected. The energy yield loss of NREL 5MW wind turbine due to the considered erosion pattern is found to be between 2.1 % and 2.6 % using measured and computed force data for the nominal and eroded



outboard blade airfoil. A parametric analysis of the cavity geometry suggests that the geometry of the cavity edge has a much larger impact on aerodynamic performance than the cavity depth. Saenz et al. (2022) measured eroded blades after several years of operation and performed a statistical study of the different sizes, shapes and locations of erosion. They were studied using CFD and the effect over the NREL 5 MW computed. The conclusion was that as closer to the leading edges and as sharper the erosion corners the most harmful effect over AEP was obtained and quantified as 3% reduction. Vimalakanthan et al. (2022) presented combined transition and rough CFD simulations of NACA 63<sub>3</sub>418 airfoil and the CFD modelling of an actual eroded blade. The conclusion of the study was that the calibrated CFD model for modeling flow transition accounting roughness shows good agreement of the aerodynamic forces for airfoils with leading-edge roughness heights in the order of 140-200  $\mu\text{m}$  when comparing with the experiments, while showing poor agreement for smaller roughness heights in the order of 100  $\mu\text{m}$ . The study indicated that up to 3.3 % reduction in AEP can be expected when the LE shape is degraded by 0.8 % of the chord, based on the NREL 5 MW wind turbine.

Besides the studies needed to characterize the effect of roughness or erosion over airfoil performance, mitigation measures with aerodynamic devices have been designed and optimized to improve blade performance. One of the most used aerodynamic devices for this purpose are Vortex Generators (VGs). VGs were used traditionally in the root area of the blades to improve the performance of the thick airfoils located in that zone. More recently vortex generators are being included in the tip area of the blades to improve efficiency in rough or eroded conditions. VGs are designed to create vorticity on the blade surface mixing high momentum zones of the upper part of the boundary layer with low momentum zones near the surface resulting in a velocity profile less prone to separation. Gutiérrez et al. (2020) worked on the definition of mitigation measures to reduce the harmful effect of roughness and an experimental study was presented. It was concluded that the increment in drag produced by VGs is negligible compared to the already present by roughness. There is not a significant change in drag due to the usage of VGs on the pressure side Hansen et al. (2016) proposed an aerodynamically shaped VG that was manufactured and tested in the wind tunnel. It was added to a DU-91-W2-250 airfoil and an efficiency increase was observed with regard to conventional vortex generators from 3.6 % to 16.36 %. With regard to simulation methodologies, when simulating VGs both fully resolved and modelling approaches are used. Seel et al. (2022) presented a comparison of performance of the use of Bay model versus the fully resolved approach when computing VGs. The agreement in terms of lift and pressure distribution is very good whereas the drag is underestimated by the BAY model

In terms of power production, Fernandez-Gamiz et al. (2017) studied in their work the energy production increase of NREL 5 MW wind turbine using the blade element momentum theory and concluding that an overall increase of 3.85 % on the average wind turbine power output can be found when using VGs and gurney flaps . These VGs where located in the blade root and mid span area and no erosion or surface roughness were included in the simulations.

Skrzypiński et al. (2020) studied the effect over AEP of retrofitting blades affected by surface roughness using VGs and determined experimentally a gain of 3.3 % and 2.8 % predicted with and engineering tool.

This study is organized as follows: first, CFD simulations of the NACA 63<sub>3</sub>418 airfoil have been performed in several surface conditions (clean, rough, pits and extreme loss of material). Then, CENER 's low drag VGs are described and the CFD simulations of blade sections for the studied surface conditions including VGs are shown. Finally, the annual energy production



of a reference 2.5 MW wind turbine is evaluated to define the effect of roughness or erosion over AEP and to estimate how  
95 much of these losses can be recovered by the installation of low drag VGs over the blade surface.

## 2 CFD simulations of rough and eroded blades

In the following subsections, simulation results for a large roughness level case and different typologies of erosion are exposed.  
The different simulations results are compared in terms of blade section performance.

### 2.1 NACA 63<sub>3</sub>418 airfoil CFD simulations for a roughness level of P40 (423 μm)

100 In this section, the simulations for the NACA 63<sub>3</sub>418 airfoil are presented for  $Re = 3 \cdot 10^6$ . The simulations were performed  
in clean and rough blade surface conditions with OpenFOAM v8 and the mesh was created using ICEMCFD. The number of  
nodes in the airfoil are 434 and the minimum size of the elements close to the surface is  $5e^{-6}$  m for the clean cases mesh in  
order to obtain  $y^+$  value below 1 to ensure the proper performance of the turbulent model. On the other hand, for the rough  
cases, the  $y^+$  values close to the airfoil surface are around 30, these  $y^+$  values are needed for the correct performance of the  
105 roughness model. The roughness model used is the one included in OpenFOAM v8 based on Cebeci (1977). This model applies  
modified logarithmic wall functions for  $y^+$  over 11.25. Going up to a  $y^+$  of 30 avoids the uncertainty of being in the buffer  
layer region which doesn't present a logarithmic behaviour with regards to  $U^+$ .

Clean cases are computed using the eN and the k-kl-w transition model. The eN transition method from van Ingen (2008)  
to simulate clean conditions is implemented in OpenFoam v8 by modifying the turbulence model intermittency factor and  
110 transition location for each angle of attack is imposed through a connection with the panel method XFOIL Drela (1989). The  
k-kl-w transition model is the one available in OpenFoam Walters and Cokljat (2008). In the rough cases the airfoil chord  
covered with rough elements is 15 % both on lower and upper sides on the leading edge zone. The roughness selected is P40  
(423 μm) using in this case the equivalent sand grain value of  $h_s = 5e^{-3}$  to compare with the experimental results measured  
in the IRPWind Joint Experiments Project Pires (2018) . A more extended evaluation of rough simulations was presented in  
115 Méndez and Pires (2022) where several roughness models and roughness sizes were evaluated. These polar curves for the clean  
and rough cases will be used to compute the AEP for a reference wind turbine in Section 4 . Figure 1 compares the airfoil lift  
coefficient, drag coefficient and efficiency both in clean (transitional computation with the k-kl-w model) and rough cases (  
comparing computations and experiments). It is observed that the CFD results reproduce accurately the experiments. A light  
over-prediction of the stall area in the lift coefficient for the clean conditions is observed.

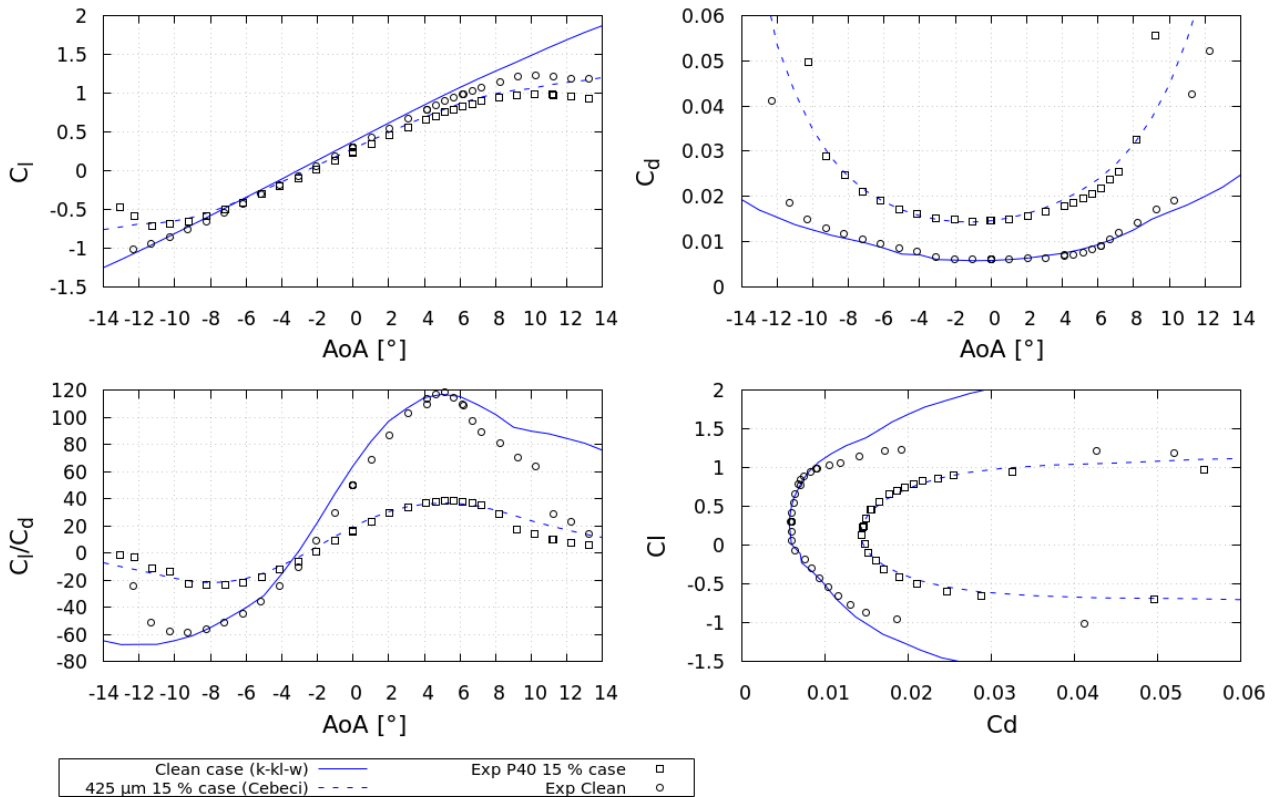


**Figure 1.** Lift, drag, efficiency and polar curves for the clean and rough conditions. Experiments for clean and rough ( $425 \mu\text{m}$  15 %) cases. NACA 63<sub>3</sub>418  $\text{Re} = 3 \cdot 10^6$ .

120 In order to justify the selection of the k-kl-w transition model as baseline in this work a comparison of the eN and k-kl-w  
 method is presented in Fig. 2 comparing with the experiments available from Pires (2018). In addition structured meshes (S-M)  
 and unstructured meshes (U-M) are compared. It is observed that lift coefficient is well predicted with the two transition models  
 and for the different meshing techniques and that they lead to differences in the drag force prediction. The structured mesh  
 with the k-kl-w method is the one that better predicts the maximum lift to drag ratio so far its selection among the different  
 125 options available is supported by these simulations. Moreover in Fig. 3 the friction coefficient for the k-kl-w and eN transition  
 models for the structured mesh are compared for three different angles of attack. The transition locations from XFOIL both  
 in the lower and upper sides of the airfoil are marked with vertical lines. This comparison demonstrates how the transition  
 location prediction by the k-kl-w method matches the one predicted with the eN transition method.

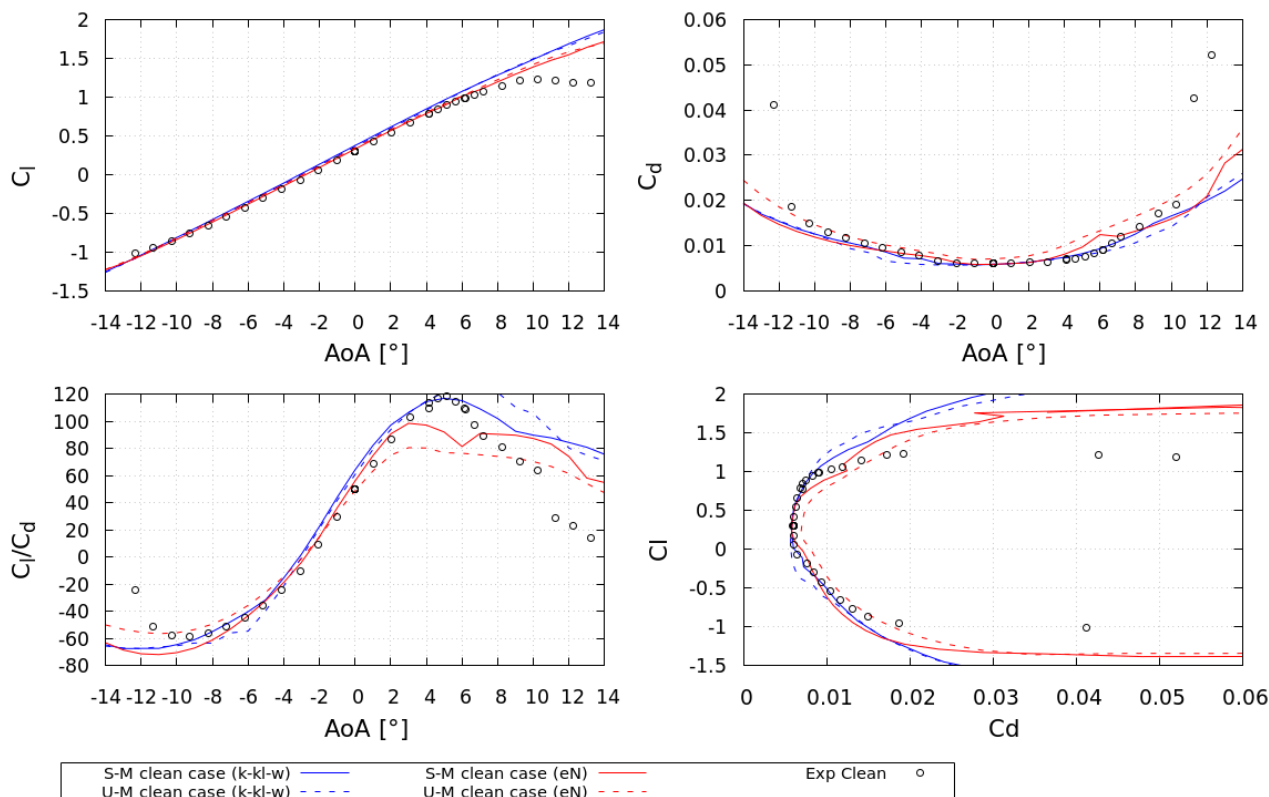


**Figure 2.** Lift, drag, efficiency and polar curves for the clean cases with k-kl-w and eN turbulence models. Experiments for clean case included. NACA 633418  $Re = 3 \cdot 10^6$ .

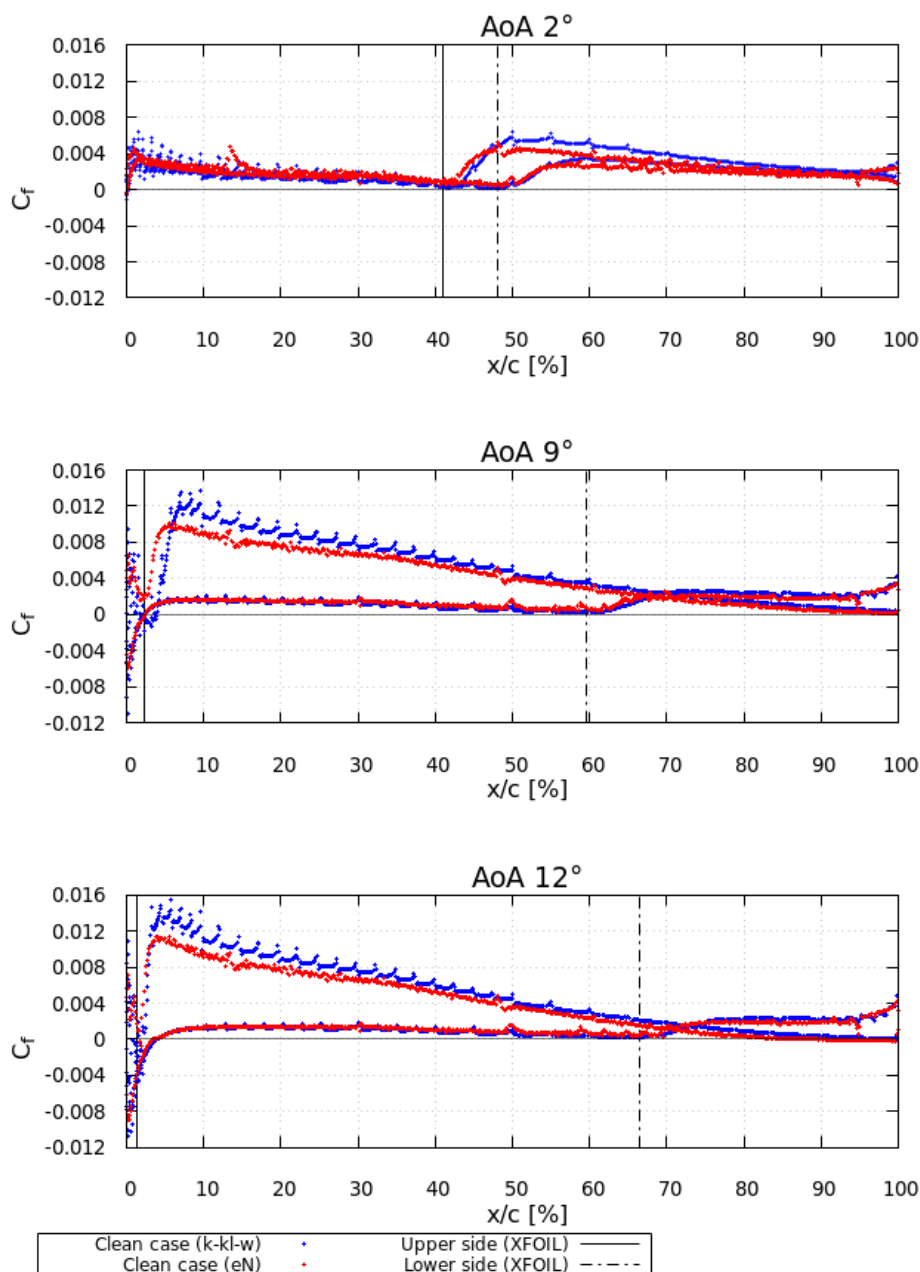


**Figure 3.** Skin friction coefficients for the clean cases with k-kl-w and eN turbulence models. Transition from laminar layer to turbulent layer. NACA 633418  $Re = 3 \cdot 10^6$ .

The accurate prediction of airfoil performance for high rough elements requires of the proper roughness model and mesh. Figure 4 shows the pressure coefficient for three different angles of attack 0°, 4° and 9°. The computations and the experiments from Pires (2018) are compared. It is observed that the pressure over the airfoil surface value is affected by the end of the

roughness area (15 % of the airfoil chord) and that the experimental pressure coefficients are predicted accurately for low and high angles of attack. These figures demonstrate that the roughness model used in this work is suitable for the simulation of very high rough elements even for high angles of attack.

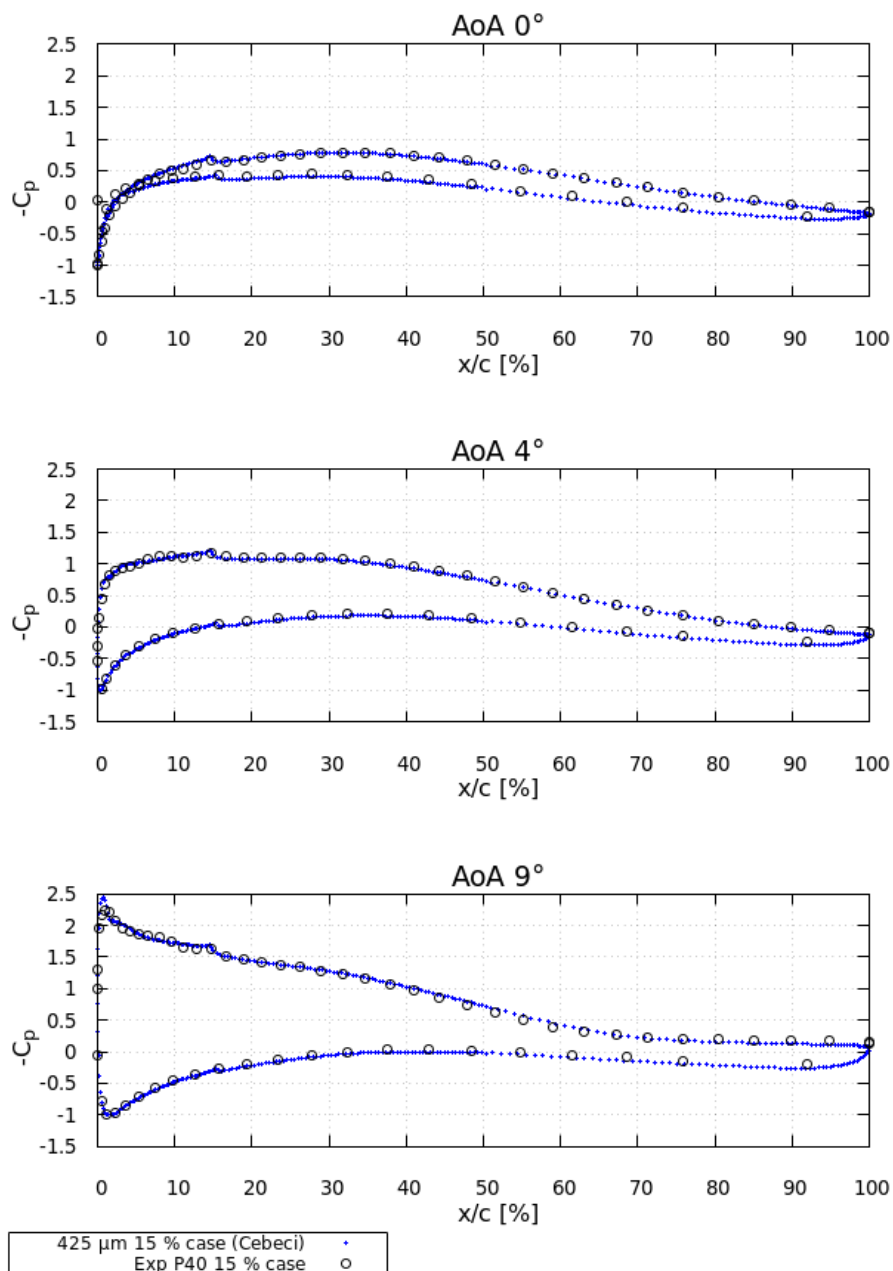


**Figure 4.** Pressure coefficient for angles of attack 0, 4 and 9 °. Simulations and experiments.



## 135 2.2 NACA 63<sub>3</sub>418 airfoil CFD simulations with surface erosion

Two different erosion types are selected and simulated in this study. They are inspired in the ones identified in Campobasso et al. (2022) and Saenz et al. (2022) and they consist in pit and gauges (Typology 1) and in an extreme loss of material (Typology 2). Both erosion types affect the airfoil leading edge area (15 % of the airfoil chord both in the upper and lower surfaces). Typology 1 erosion consists of 26 pits with a maximum depth of 2.5 mm and the Typology 2 (extreme loss of material) consists of a loss of 5mm of the coating. The CFD simulations of the two erosion types use 3D meshes since the pits distribution of Typology 1  
140 of 5mm of the coating. The CFD simulations of the two erosion types use 3D meshes since the pits distribution of Typology 1 erosion along the airfoil section changes heterogeneously, and with the aim of introducing the VGs in the subsequent parts of this study. The meshes for both cases are shown in Fig. 5 and Fig. 6.

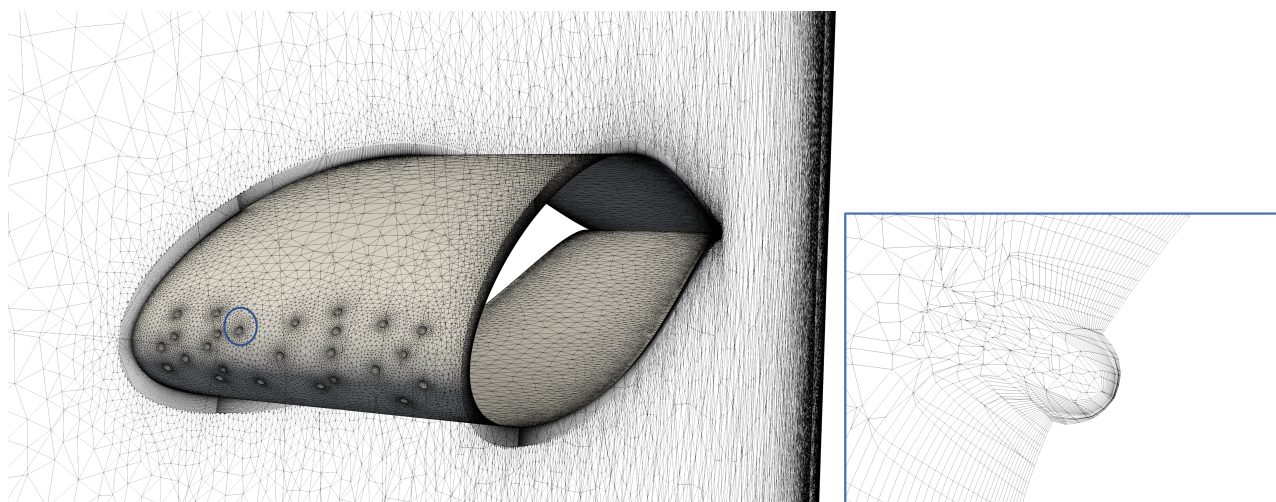


**Figure 5.** Mesh for computing erosion pits in the leading edge area. Erosion Typology 1. A zoom in the neighbourhood of the pit area is included.

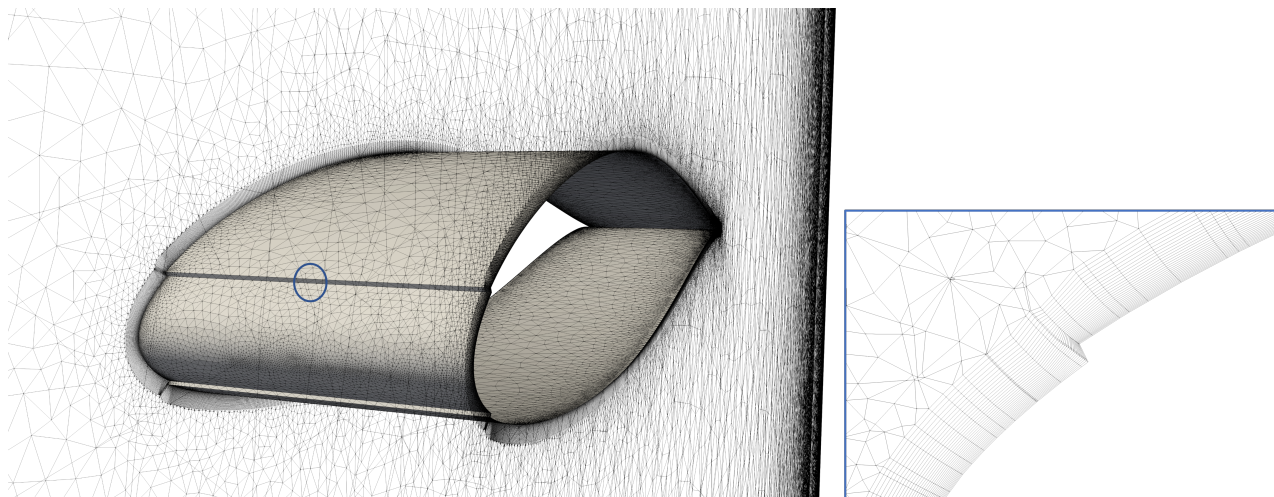


**Figure 6.** Mesh for computing extreme loss of material in the leading edge area. Erosion Typology 2. A zoom in the neighbourhood of the loss of material area is included.

The meshes were created with ANSYS Workbench to control the inflation layers definition in the vicinity of the airfoil eroded areas. The size of the first inflation layer is  $1.5e^{-4}$  m with an expansion ratio to achieve the  $y^+$  value around 1 necessary in  
145 OpenFOAM to have a proper performance of the turbulence model. Figure 7 show how the tetra elements in the mesh connect with the prismatic elements in the airfoil surface.

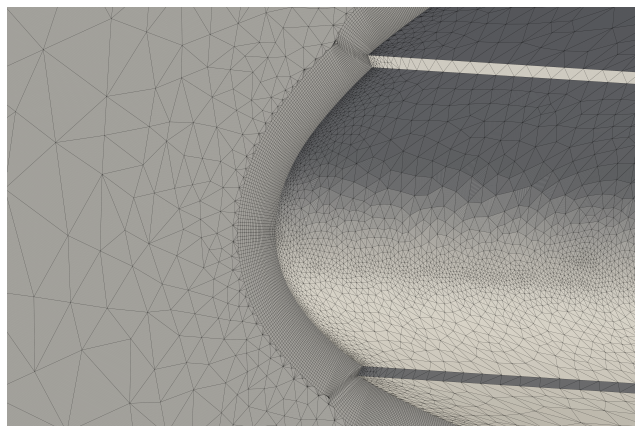


**Figure 7.** Inflation layers close to the airfoil surface.

The simulations were performed for a Reynolds number of  $Re = 3 \cdot 10^6$ . Figure 8 shows the comparison of both erosion types effect over airfoil performance with regard to the clean case (k-kl-w transition model). The simulations for the eroded cases are performed using the SST k-w turbulence model so the reference airfoil simulated with this turbulence model is included. The  
150 rough surface case is also added to use it in the comparison and discussion performed in Section 2. The airfoil performance is modified when erosion appears comparing with the undisturbed airfoil shape being erosion Typology 2 more harmful in terms

of airfoil efficiency. The lift curve slope is reduced and drag coefficient increases when erosion appears. Figures 9 and 10 show the flow field in the blade section for erosion Typology 1 and erosion Typology 2 for AoA of 12°. It is observed how erosion forces the boundary layer separation and that small pits directly affect the evolution of the boundary layer due to its location and shape.

155

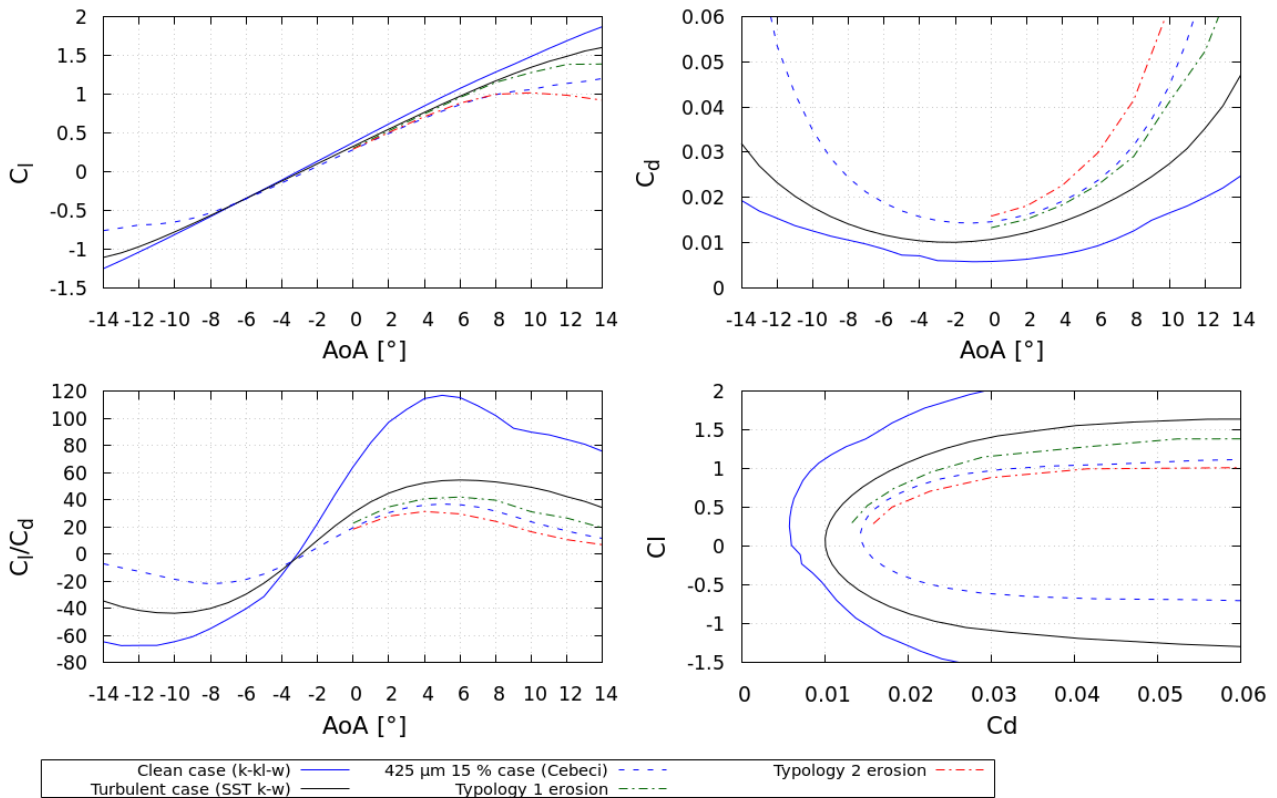


**Figure 8.** Lift, drag, efficiency and polar comparison for clean, rough (425  $\mu\text{m}$  15 %) and two erosion typologies (1 and 2). NACA 633418  $\text{Re} = 3 \cdot 10^6$ .

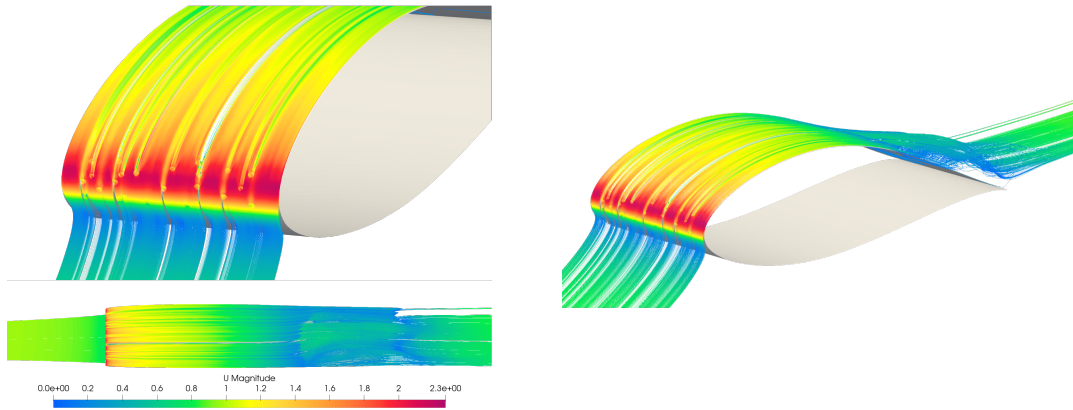


**Figure 9.** Flow field for Erosion Typology 1. CFD simulations. AoA 12°.

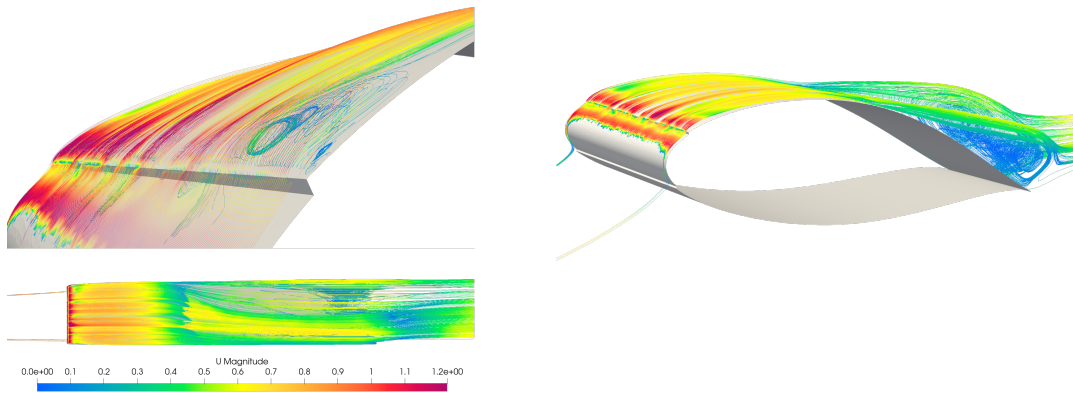


**Figure 10.** Flow field for Erosion Typology 2. CFD simulations. AoA 12°.

### 2.3 Rough and eroded airfoil performance comparison and discussion

The comparison of the effect of rough and eroded blades over airfoil performance is discussed in this section. In Fig. 8 the performance of NACA 63<sub>3</sub>418 airfoil for clean, rough and eroded conditions was shown. In addition, the performance coefficients are summarized in Table 1. The values obtained in the experimental campaign Pires (2018) are also included to provide an idea of the same comparison obtained from wind tunnel experiments. Rough surface leads to an efficiency loss of 68.54 % and erosion pits of 64.11 % and extreme loss of material of 73.24 % comparing with the clean airfoil. Erosion and roughness events have a detrimental effect over airfoil performance. Rough and Typology 1 erosion cases present similar effect over airfoil performance so it is demonstrated that high rough elements can be even worse than erosion in certain situations. The effect over airfoil efficiency predicted in the wind tunnel for the rough cases was similar to the one obtained in the computations.



**Table 1.** Summary of airfoil aerodynamic characteristics. CFD simulations and experiments NACA 63<sub>3</sub>418  $Re = 3 \cdot 10^6$ .

	$C_{d,min}$	$\alpha_{C_{d,min}}$	$C_{l,max}$	$\alpha_{C_{l,max}}$	$(C_l/C_d)_{max}$	$\alpha_{(C_l/C_d)_{max}}$	$\Delta(C_l/C_d)$ [%]
CFD Clean (k-kl-w)	0.58e-2	-1	1.87	14.00	116.96	5	-
CFD turbulent flow (SST k-w)	1.01e-2	-2	1.60	14.00	54.54	6	-53.37
CFD P40 (423 $\mu$ m) 15 %c	1.43e-2	-1	1.20	14.00	36.80	5	-68.54
CFD Erosion Typology 1	1.33e-2	0	1.39	14.00	41.98	6	-64.11
CFD Erosion Typology 2	1.59e-2	0	1.02	10.00	31.30	4	-73.24
Experimental Clean	0.64e-2	0	1.24	10.24	118.00	5	-
Experimental P40 (423 $\mu$ m) 15 %c	1.48e-2	-1	0.98	10.13	38.14	5	-67.6

### 165 3 Vortex generators used as roughness and erosion mitigation measure

VGs are passive flow control devices that are usually triangular or rectangular vanes inclined to the flow and are sized with regard to the local boundary layer thickness. VGs are known for their capability to delay separation and increase lift force on the blade. Their main drawback is the drag penalty added to the blades. In this study, a novel VG shape based on an airfoil-like cross shape is added to the blade sections in the clean, rough and eroded cases. This low drag vortex generator is used in this work to mitigate the harmful effect of the roughness and erosion types described and computed in Section 2.

#### 3.1 CENER 's low drag VGs

CENER 's low drag vortex generators are based on a 10 % thickness airfoil. The main characteristic of this airfoil is to have a low drag. The 3D geometry of CENER VG is shown in Fig. 11. A VG pair is located in the different NACA 63<sub>3</sub>418 airfoil surface status options: clean, rough, erosion Typology 1 and erosion Typology 2. CENER 's low drag VGs have been tested in the wind tunnel under the scope of the ODB (The Offshore Demonstration Blade) project. It was observed in the measurements, the use of Vortex Generators lead to an increase in lift coefficient, a slight increase in drag and an increase in efficiency

#### 3.2 Blade section including VGs meshing

CENER 's low drag VG ability to mitigate blade surface detrimental conditions has been studied in the a blade section based on the NACA 63<sub>3</sub>418 airfoil in different conditions: clean, rough, and eroded cases.

In this study, vortex generators are modelled using a fully resolved approach. That means that they are included in the 3D blade section and their geometry is meshed. The challenge associated to this approach comes from the necessity of simulating accurately the boundary layers both in the vortex generator surface and in the airfoil surface. In this work, the ANSYS Workbench has been used to mesh properly the VG and airfoil boundary layers without increasing the total number of cells in the

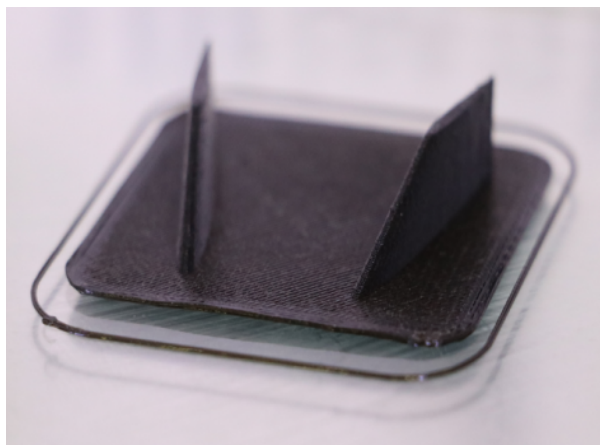


**Figure 11.** CENER's low drag vortex generator geometry.

185 mesh. The same characteristics are used to create these meshes except for the inflation layer size close to the VGs that is  $1e^{-5}$  m.

In Fig. 12 a detailed view of the mesh close to the vortex generator pair is shown. In all the cases the VGs were placed at the 30 % of the chord in order to compare the same type of magnitudes. It is necessary to remark that the VGs optimum location depends on the specific case so the use of the same position for clean, rough and erosion cases is justified only for comparing the results. For the clean surface case with VGs the total elements in the mesh are 2.75 million and 2.62 and 2.73 million for erosion Typologies 1 and 2. Figure 13 show the mesh used when VGs are modelled in the turbulent, rough, erosion Typology 1 and erosion Typology 2.

190

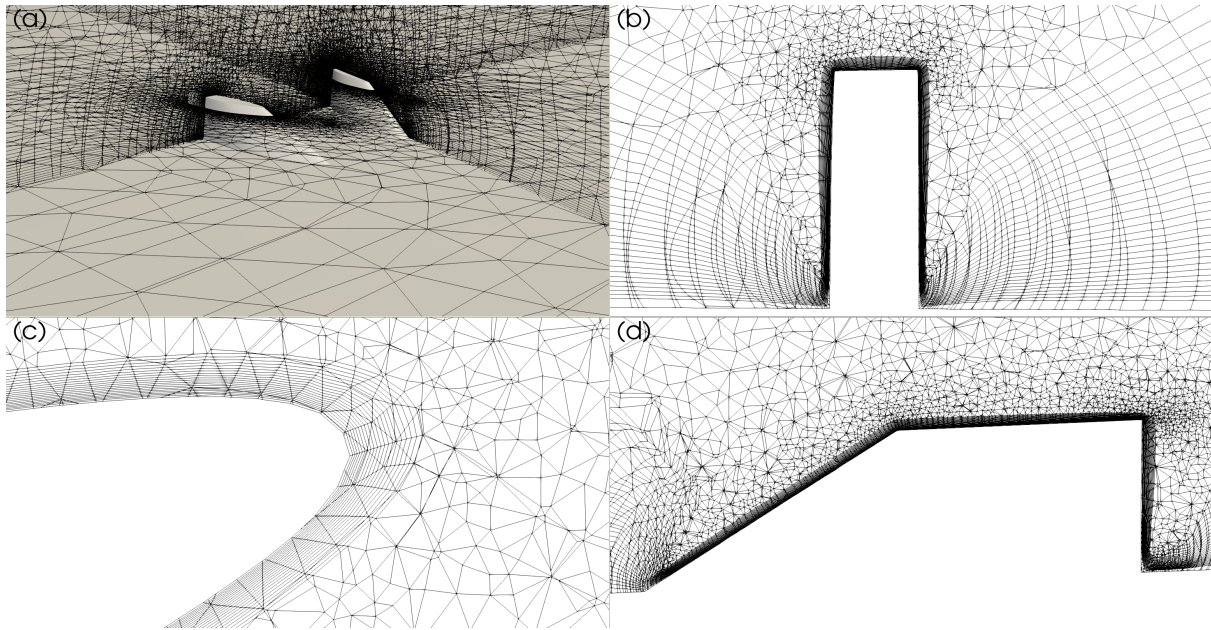


**Figure 12.** Mesh for CENER's low drag VGs.(a) Slices location, (b) 1 VG front view, (c) 1 VG top leading edge view, (d) 1 VG side view



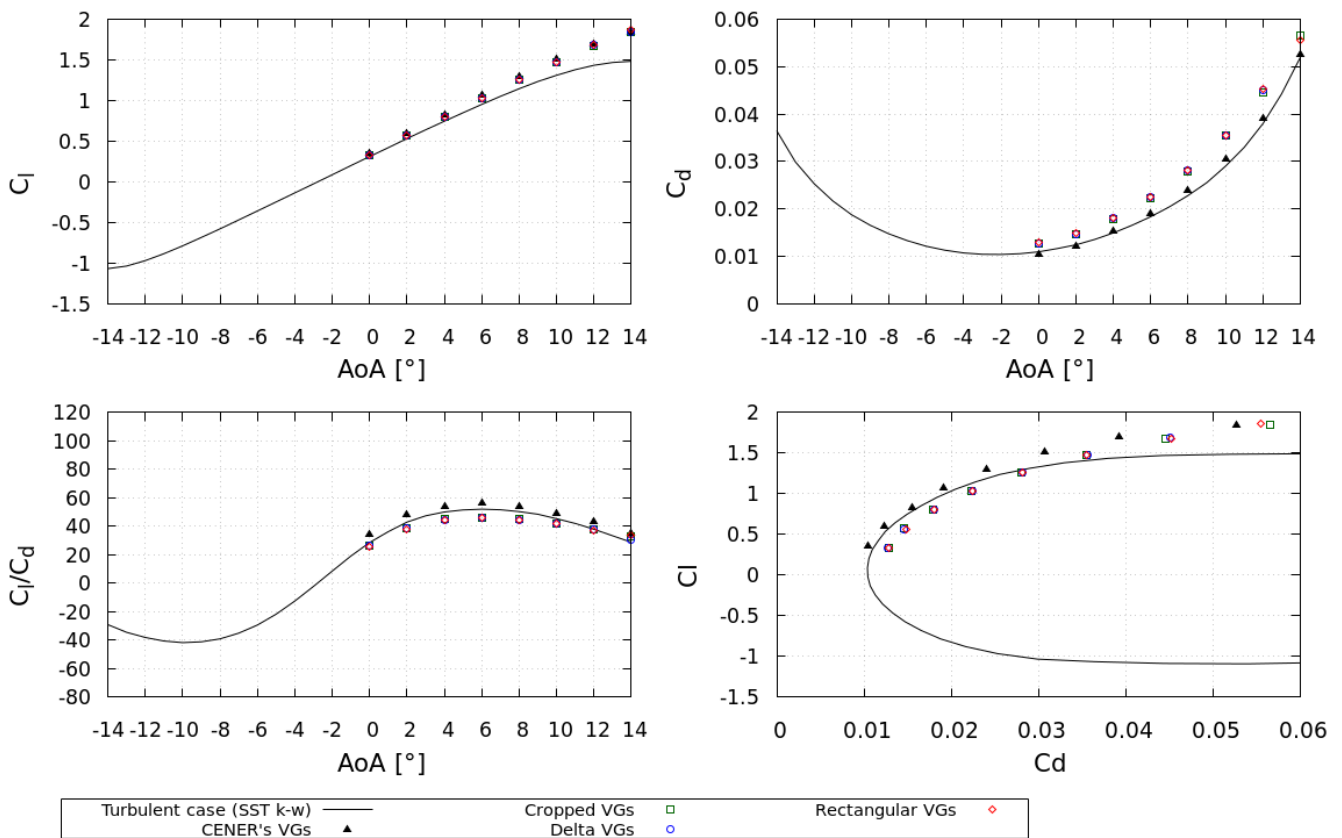
**Figure 13.** Mesh for rough (left), type 1 eroded (middle) and type 2 eroded (right) cases with CENER's Low Drag VGs.

### 3.3 CENER's low drag VGs performance comparison vs conventional VGs

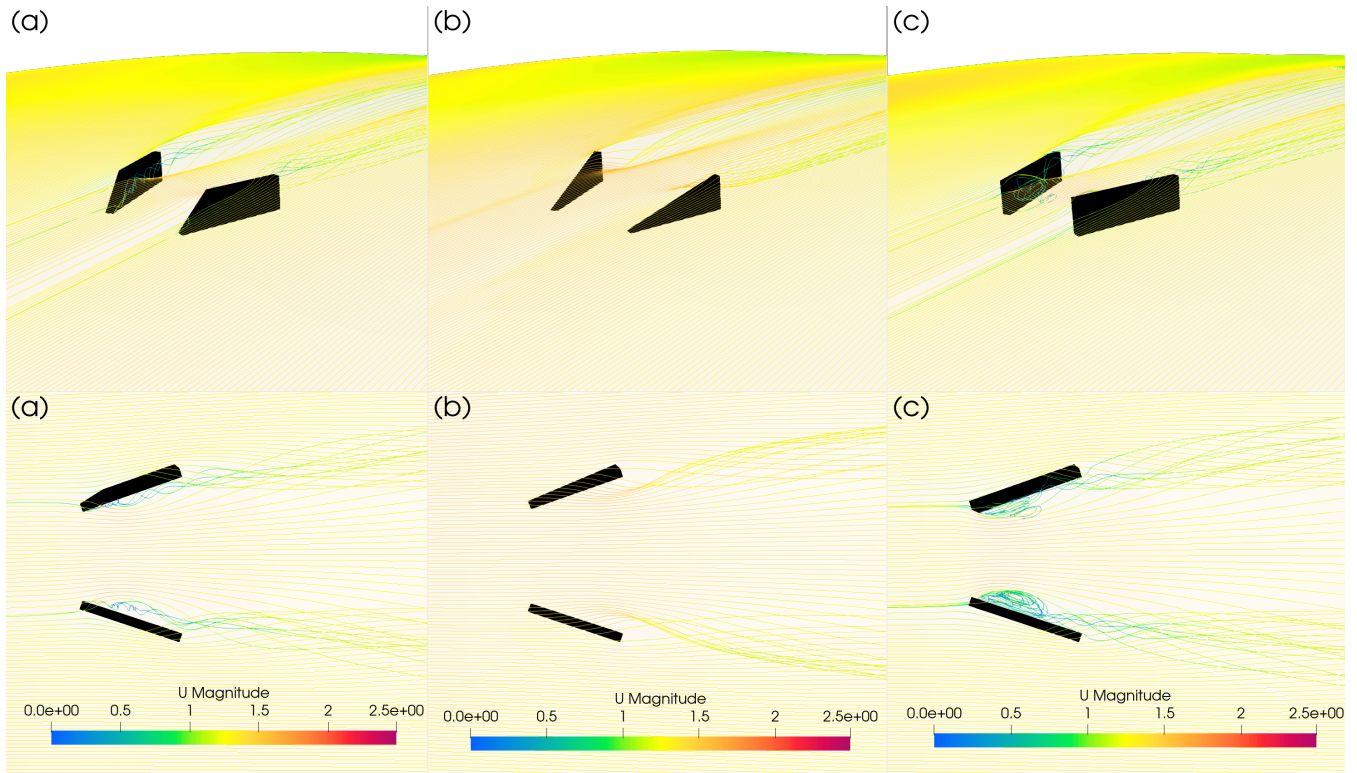
Justification of benefits of using low drag VGs is presented in Fig. 14. The performance comparison of different types of conventional VGs (cropped, delta and rectangular) with regard to CENER's low drag VGs is presented for the NACA 63<sub>3</sub>418 airfoil for a Reynolds number of  $Re = 3 \cdot 10^6$ . Lift and drag coefficient are shown as well as efficiency. For this study the VGs location has been settled making a parametric study of the best location along the airfoil chord. This location for the VGs is used in all this study. It is observed that low drag VGs present advantages with regard to conventional VGs: higher lift and lower drag that lead to an efficiency increase in the whole range of angles of attack (efficiency increase with regard to the



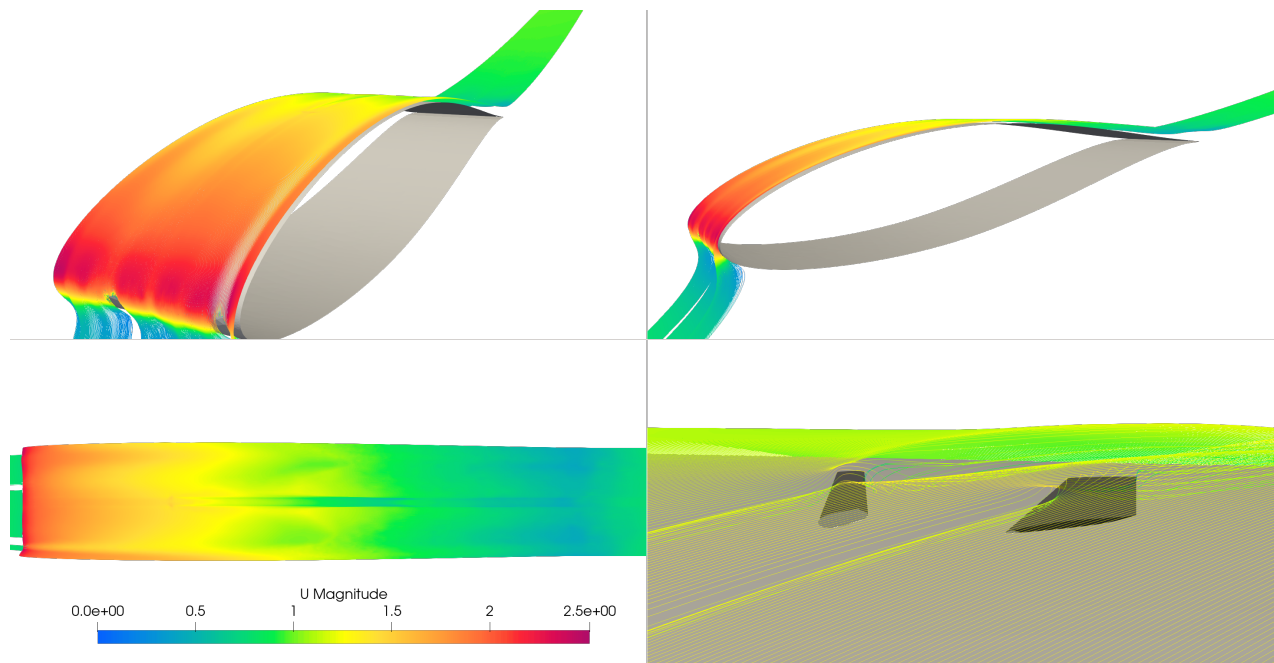
conventional VGS of 18% for the maximum efficiency angle of attack). Figure 15 show the streamlines for the three different  
 200 types of conventional VGs showing how the shape of the VG is crucial for the vortex pair creation. Figure 16 plots the flow  
 when low drag VGs are installed in a reference blade section. The VGs location and the separation location can be observed.



**Figure 14.** Lift, drag, efficiency and polar curves for turbulent conditions with CENER's vortex generators and conventional VGs (cropped, delta and rectangular) at 30% of the chord. CFD simulations. NACA 63<sub>3</sub>418  $Re = 3 \cdot 10^6$ .



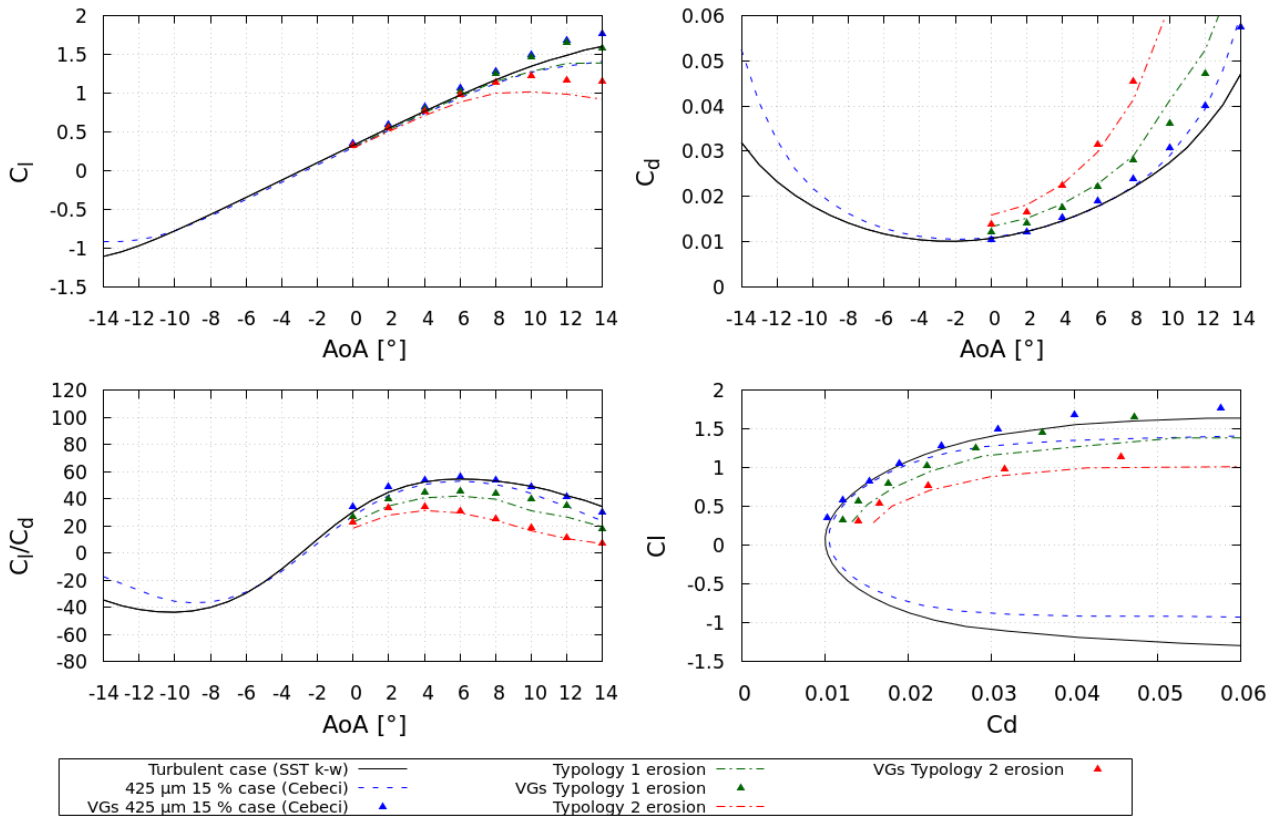
**Figure 15.** Streamlines for Cropped (a), Delta (b) and Rectangular (c) VGs.



**Figure 16.** Streamlines for CENER 's low drag VGs for the baseline airfoil case.

### 3.4 Blade section performance including Vortex Generators

The CFD simulations performed in the 3D blade sections including blade defects and low drag VGs are done with OpenFOAM v8. The blade span is 0.2 m. Figure 17 show the polar curves for the rough and two erosion types with and without VGs. The  
205 turbulent case for the undisturbed airfoil is also included for comparison. In the rough and eroded blades, the introduction of a VG leads to a lift increase and and efficiency increase. Table 2 summarize the sectional coefficients when VGs are included in the simulations, maximum efficiency variation with regard to the turbulent flow (SST k-w) case in the reference blade is included. They are made 2D using the blade sectional forces and the blade span. It is very important to highlight that the introduction of VGs over the airfoil surface lead to a recovery of the airfoil efficiency with regard to the rough and eroded  
210 conditions.



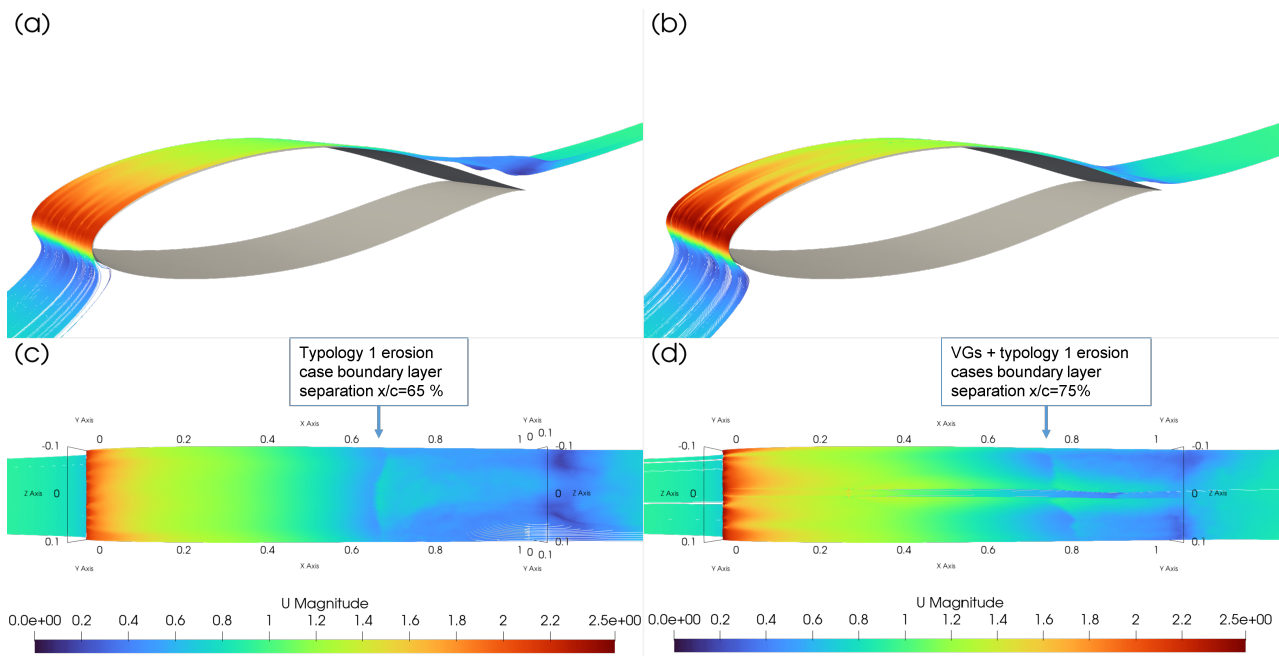
**Figure 17.** Lift, drag, efficiency and polar curves for rough and eroded conditions without and with CENER’s low drag VGs at 30 % of the chord. CFD simulations. NACA 63<sub>3</sub>418  $Re = 3 \cdot 10^6$ .

Figure 18 compares the effect of adding low drag VGs when the blade sections has and erosion Typology 1 (pits). In (a) no low drag VGs are included and flow separation occurs at 65% of the airfoil chord (c). When the low drag VGs are included the flow is much attached to the surface (b) and separation occurs at 75% of the airfoil chord. This effect can also be observed in Fig. 19 where the friction coefficient is plotted for Typology 1 erosion, for Typology 1 erosion with low drag VGs and also for the turbulent case. Again, the separation delay due to the use of VGs is verified.



**Table 2.** Summary of section aerodynamic characteristics. CFD simulations without and with VGs. NACA 63<sub>3</sub>418  $Re = 3 \cdot 10^6$ .

	$C_{d,min}$	$\alpha_{C_{d,min}}$	$C_{l,max}$	$\alpha_{C_{l,max}}$	$(C_l/C_d)_{max}$	$\alpha_{(C_l/C_d)_{max}}$	$\Delta(C_l/C_d)$ [%]
1a CFD turbulent flow	1.01e-2	-2	1.60	14	54.54	6	-
1b CFD turbulent flow + VG	1.05e-2	0	1.84	14	56.02	6	+2.71
2a CFD P40 15%c	1.43e-2	-1	1.20	14	36.80	5	-32.53
2b CFD P40 15%c + VG	0.58e-2	0	1.60	12	44.35	6	-18.68
3a CFD Erosion Typology 1	1.33e-2	0	1.39	14	41.98	6	-23.03
3b CFD Erosion Typology 1 + VG	1.22e-2	0	1.66	12	47.15	6	-13.55
4a CFD Erosion Typology 2	1.59e-2	0	1.02	10	31.30	4	-42.61
4b CFD Erosion Typology 2 + VG	1.40e-2	0	1.23	10	34.43	4	-36.87



**Figure 18.** NACA 63<sub>3</sub>418 with and without CENER's VGs streamlines at AoA 12°. (a) NACA 63<sub>3</sub>418 side view. (b) NACA 63<sub>3</sub>418 with VG's side view. (c) NACA 63<sub>3</sub>418 top view. (d) NACA 63<sub>3</sub>418 with VGs top view. Erosion Typology 1

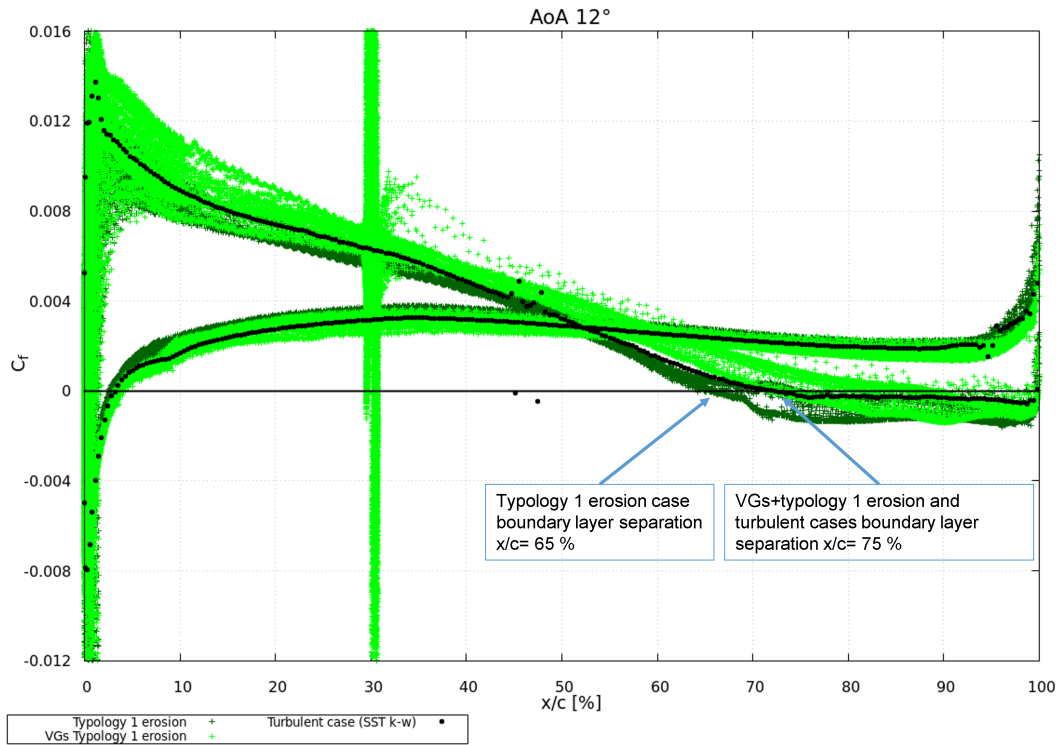


**Figure 19.** Skin friction coefficient for erosion Typology 1, erosion Typology 1 + VGs and turbulent cases. NACA 63<sub>3</sub>418  $Re = 3 \cdot 10^6$  AoA 12°.

#### 4 Effect of roughness or erosion over Annual Energy Production. Evaluation of the improvement with the use of VGs

In this section the effect over a reference wind turbine AEP has been evaluated. This evaluation is performed over clean blades, rough and eroded blades and also in the three configurations when CENER's Low Drag VGs are installed.

The reference blade selected is a virtual blade designed using the optimization code BladeOASIS that mimic the blade features of the N80 2.5 MW wind turbine used in the Joint Experiments Pires (2018). BladeOASIS uses a genetic algorithm optimization to design blade aerodynamics and structure complying with the design restrictions and objective functions. A detailed description of how this blade has been conceived can be found in Méndez and Pires (2022), but essentially the online available information of the N80 wind turbine is used to create a model that fits the online available power curve. This wind turbine has been designed using the clean polar curve of the NACA 63<sub>3</sub>418 computed in Section 2. The AEP of that case is selected as the reference energy production to evaluate the effect of the rest of configurations. Afterwards, the rough, eroded, rough with VGs and eroded with VGs are introduced in the evaluation using the corresponding polar curves to obtain their



effect over AEP. The last 5 meters of the blade (from 32 to 37 m length) and the 15 % of the blade chord both in the lower and upper side are affected by roughness or the two erosion types. A summary of the results is shown in Table 3. It is observed how the damages over the blade surface have a dramatic effect over power production and that the use of VGs can recover up to 1.5 % of the AEP which could lead to an increase in power production revenues until the blade repair maneuvers can be done.

**Table 3.** AEP in the different blade conditions evaluated in the N80 2.5 MW Digital Twin.

Blade type	AEP decrease [%]
Reference Blade	-
Rough blade	-3.48
Erosion Type 1 Blade	-5.19
Erosion Type 2 Blade	-8.97
Rough Blade + VGs	-2.63
Erosion Type 1 Blade + VGs	-3.99
Erosion Type 2 Blade + VGs	-7.45

## 5 Conclusions

There are several interesting conclusions that can be found in this work:

- High fidelity simulations of airfoil performance including extreme surface roughness match accurately experiments in the NACA 63<sub>3</sub>418 airfoil.
- Cebeci and Bradshaw roughness model works properly for the high size roughness levels of 423  $\mu\text{m}$ .
- Different typologies of erosion can be fully resolved with CFD. The geometry of the eroded cases is meshed with an hybrid ANSYS Workbench mesh combining tetras and prismatic elements to ensure quality of the results with affordable computational times.
- The effect over airfoil efficiency computed is 68 % and 64 % and 73 % reduction for rough and eroded cases (Typology 1 and 2) respectively. Similar effect is observed in the experiments for rough cases with the same elements size
- VGs introduced over airfoils or blade sections lead to lift and drag increase.
- The AEP decrease predicted computationally when roughness or erosion appear varies from 3.48 % to 8.97 %.
- The introduction of VGs over the blade section lead to an AEP recovery of 1.5 % in the Digital Twin of the 2.5 MW wind turbine. Further studies will be done in bigger wind turbines.
- The worse the blade defects, the more AEP recovery is expected with the introduction of vortex generators.



- All the simulations presented in this work are done for a Reynolds number of  $3 \cdot 10^6$  to be consistent with the experimental campaign available. Multi-megawatt wind turbines operation conditions lead to bigger Reynolds numbers so a recommendation is to test the effect over models, meshing techniques and VGs operation for Reynolds numbers up to  $12 \cdot 10^6$ .
- 250 – The effect of blade damages over wind turbine AEP prediction is still a manual process that relies on the researcher skills both in the model and mesh tuning. Automatising this process is needed to provide accurate information and helpful tools to wind farm operators.
- The fully resolved approach can be used to compute blade sections including VGs but is necessary to create very elaborated meshes to have affordable computational times
- 255 – Results are fully dependent on the VG size, location and angle. A parametric study should be made for each specific blade and airfoil to ensure the optimal performance of the VGs
- CENER's Low drag VGs presented a better performance than conventional shaped VGs of equal size for the NACA 63<sub>3</sub>418 airfoil. Efficiency increase with regard to the conventional VGs cases of 18% for the maximum efficiency angle of attack in the cases without roughness or erosion
- 260 – A reference blade with VGs installed from the factory leads to an AEP reduction that could be economically justified by the recovery of power production when the blades are eroded or rough
- There are still many sources of uncertainty regarding the CFD airfoil simulations and experimental results, specially at high angles of attack. The simulations are usually performed with steady state temporal schemes in order to get an affordable computational cost whereas the flow at high angles of attack is unsteady.
- 265 *Author contributions.* David Bretos: CFD computations, Methodology, Validation, Visualization, Writing. Beatriz Mendez: CFD computations, Methodology, Validation, Visualization, Funding acquisition, Supervision, Visualization, Writing – original draft preparation.

*Competing interests.* The authors declare that they have no conflict of interest.



## References

- Bak, C., Forsting, A. M., and Sorensen, N. N.: The influence of leading edge roughness, rotor control and wind climate on the loss in energy  
270 production, *Journal of Physics: Conference Series*, 1618, 052 050, <https://doi.org/10.1088/1742-6596/1618/5/052050>, 2020.
- Campobasso, M. S., Castorrini, A., Cappugi, L., and Bonfiglioli, A.: Experimentally validated three-dimensional computational aerodynam-  
ics of wind turbine blade sections featuring leading edge erosion cavities, *Wind Energy*, 25, 168–189, <https://doi.org/10.1002/we.2666>,  
2022.
- Cebeci, T., B. P.: *Momentum Transfer in Boundary Layers*, Hemisphere Publishing Corporation, 1977.
- 275 Drela, M.: XFOIL: An Analysis and Design System for Low Reynolds Number Airfoils, in: *Low Reynolds Number Aerodynamics*, edited  
by Mueller, T. J., pp. 1–12, Springer Berlin Heidelberg, Berlin, Heidelberg, 1989.
- Ehrmann, R., White, E., Maniaci, D., Chow, R., Langel, C., and Dam, C.: Realistic Leading-Edge Roughness Effects on Airfoil Performance,  
<https://doi.org/10.2514/6.2013-2800>, 2013.
- Fernandez-Gamiz, U., Zulueta, E., Boyano, A., Ansoategui, I., and Uriarte, I.: Five Megawatt Wind Turbine Power Output Improvements by  
280 Passive Flow Control Devices, *Energies*, 10, <https://doi.org/10.3390/en10060742>, 2017.
- Gutiérrez, R., Llórente, E., Echeverría, F., and Ragni, D.: Wind tunnel tests for vortex generators mitigating leading-edge roughness on a  
30% thick airfoil, *Journal of Physics: Conference Series*, 1618, 052 058, <https://doi.org/10.1088/1742-6596/1618/5/052058>, 2020.
- Hansen, M., Velte, C., Øye, S., Hansen, R., Sørensen, N., Madsen, J., and Mikkelsen, R.: Aerodynamically shaped vortex generators, *Wind  
Energy*, 19, 563–567, <https://doi.org/10.1002/we.1842>, 2016.
- 285 Kruse, E., Sørensen, N. N., and Bak, C.: A two-dimensional quantitative parametric investigation of simplified surface imperfections on the  
aerodynamic characteristics of a NACA 633-418 airfoil, *Wind Energy*, 24, 310–322, <https://doi.org/10.1002/we.2573>, 2021.
- Kruse, E. K., Sørensen, N., Bak, C., and Nielsen, M. S.: CFD simulations and evaluation of applicability of a wall roughness model applied  
on a NACA 633-418 airfoil, *Wind Energy*, 23, 2056–2067, <https://doi.org/10.1002/we.2545>, 2020.
- Maniaci, D., Westergaard, C., Hsieh, A., and Paquette, J.: Uncertainty Quantification of Leading Edge Erosion Impacts on Wind Turbine  
290 Performance, *Journal of Physics: Conference Series*, 1618, 052 082, <https://doi.org/10.1088/1742-6596/1618/5/052082>, 2020.
- Méndez, B. and Pires, O.: Impact of high size distributed roughness elements on wind turbine performance, *Journal of Physics: Conference  
Series*, 2265, 032 027, <https://doi.org/10.1088/1742-6596/2265/3/032027>, 2022.
- Pires, O. e. a.: Experimental investigation of Surface Roughness effects and Transition on Wind Turbine performance., *IOP Conf. Series:  
Journal of Physics: Conf. Series* 1037 052018, 2018.
- 295 Saenz, E., Mendez, B., and Muñoz, A.: Effect of erosion morphology on wind turbine production losses, *Journal of Physics: Conference  
Series*, 2265, 032 059, <https://doi.org/10.1088/1742-6596/2265/3/032059>, 2022.
- Seel, F., Blazejewski, L., Lutz, T., and Krämer, E.: Numerical Assessment of a BAY-Type Model for different Vortex Generator Shapes Ap-  
plied on a Wind Turbine Airfoil, *Journal of Physics: Conference Series*, 2265, 032 001, <https://doi.org/10.1088/1742-6596/2265/3/032001>,  
2022.
- 300 Skrzypiński, W., Gaunaa, M., Bak, C., Junker, B., Brønnum, N. B., and Kruse, E. K.: Increase in the annual energy production due to a  
retrofit of vortex generators on blades, *Wind Energy*, 23, 617–626, <https://doi.org/10.1002/we.2446>, 2020.
- Standish, K., Rimmington, P., Laursen, J., Paulsen, H., and Nielsen, D.: Computational Predictions of Airfoil Roughness Sensitivity.
- van Ingen, J.: *The eN Method for Transition Prediction. Historical Review of Work at TU Delft*, 2008.

<https://doi.org/10.5194/wes-2023-8>  
Preprint. Discussion started: 9 February 2023  
© Author(s) 2023. CC BY 4.0 License.



305 Vimalakanthan, K., van der Mijle Meijer, H., Bakhmet, I., and Schepers, G.: CFD modeling of actual eroded wind turbine blade, Wind Energy Science Discussions, 2022, 1–35, <https://doi.org/10.5194/wes-2022-65>, 2022.

Walters, D. K. and Cokljat, D.: A Three-Equation Eddy-Viscosity Model for Reynolds-Averaged Navier–Stokes Simulations of Transitional Flow, Journal of Fluids Engineering, 130, <https://doi.org/10.1115/1.2979230>, 121401, 2008.